Journal of Magnetism and Magnetic Materials 400 (2016) 163–167

Contents lists available at ScienceDirect

Journal of Magnetism and Magnetic Materials

journal homepage: www.elsevier.com/locate/jmmm

Effective exchange fields in spin-torque resonance of magnetic insulators

Takahiro Chiba [a,*], Gerrit E.W. Bauer [a,b,c], Saburo Takahashi [a]

[a] Institute for Materials Research, Tohoku University, Sendai 980-8577, Japan
[b] WPI-AIMR, Tohoku University, Sendai, Miyagi 980-8577, Japan
[c] Kavli Institute of NanoScience, Delft University of Technology, Lorentzweg 1, 2628 CJ Delft, The Netherlands

ARTICLE INFO

Article history:
Received 20 June 2015
Received in revised form
17 July 2015
Accepted 18 July 2015
Available online 20 July 2015

Keywords:
Yttrium iron garnet
Spin-torque ferromagnetic resonance
Spin-Hall magnetoresistance
Spin-mixing conductance

ABSTRACT

We report additional results on the spin-torque ferromagnetic resonance (ST-FMR) of a bilayer system made from a magnetic insulator such as $Y_3Fe_5O_{12}$ (YIG) and a heavy normal metal such as Pt in terms of the interface spin-mixing conductance and including spin pumping. We analyze experimental ST-FMR spectra for out-of-plane and in-plane magnetization configurations in terms of an anisotropic imaginary part G_i of the mixing conductance (or interface effective field). The estimated ratio between imaginary and real parts $G_i/G_r \lesssim 0.3$ is sensitive to an (unknown) phase shift between microwave current bias and associated Oersted field.

1. Introduction

The ferrimagnetic insulator (FI) $Y_3Fe_5O_{12}$ (YIG) can be electrically [1] and thermally [2] activated by attached heavy normal metals (NM) such as Pt with large spin Hall angle. We proposed to employ spin-torque ferromagnetic resonance (ST-FMR) [3,4] to study magnetic insulators [5,6] by making use of the spin Hall magnetoresistance (SMR) [7,8] (see Fig. 1). Iguchi et al. [9] reported negligibly small effects due to SMR when subjecting a YIG‖Pt bilayer to FMR conditions in a microwave cavity. On the other hand, Schreier et al. [10] and Sklenar et al. [11] do find SMR rectification voltages when driving a microwave current through the Pt. The first collaboration interprets the differences of the observed spectra in samples with different thicknesses of both Pt and YIG in terms of the competition between Oersted fields, spin–orbit torques, and spin pumping [10], in good agreement with theoretical predictions [5]. The second group focuses on the ST-FMR measurement in out-of-plane (oop) magnetization configurations and reports a SMR rectification that is affected by an additional effective field [11].

The spin transport through the interface between ferromagnets and normal-metals is governed by the complex spin-mixing conductance $G^{\uparrow\downarrow} = G_r + iG_i$ (per unit area of the interface) [12]. The predicted large G_r for the interfaces between YIG and simple metals [13] has been confirmed by experiments [14,15]. G_i can be interpreted as an effective exchange field between magnetization and a spin accumulation in an attached NM, which in the absence of spin–orbit interaction is usually much smaller than the real part. However, field-like spin–orbit torques have been found in metallic structures [16,17]. In the YIG|Pt system the SMR for out-of-plane magnetizations has been interpreted in terms of a $G_i \ll G_r$ [18,19].

Here we compute ST-FMR signals of ferro- or ferrimagnetic insulators attached to a heavy normal metal by modeling a field-like torque (including ac spin pumping contributions) allowing for a large $|G_i|$ [6]. In Ref. [10] the phase between Oersted field and applied microwave current was assumed to suffer a phase shift due to unknown origins. We show that the experiments with an adjustable phase can be also explained by introducing an anisotropic interface field-like torque. We fit the observed frequency-dependent voltages [10] for nearly perpendicular and in-plane magnetization configurations in terms of an adjustable G_i for an ultra thin film of YIG. We find an anisotropic G_i that is larger for the out-of-plane than the in-plane magnetization configuration, which is still smaller than the real part G_r, however. The sizable G_i (of the order of G_r) reported for mostly out-of-plane magnetization configurations [11] is qualitatively consistent with our results.

2. Spin-torque ferromagnetic resonance

The ST-FMR technique should be distinguished from the electrical (inverse spin Hall effect) detection of conventional FMR in

* Corresponding author.
E-mail address: t.chiba@imr.tohoku.ac.jp (T. Chiba).

http://dx.doi.org/10.1016/j.jmmm.2015.07.058
0304-8853/

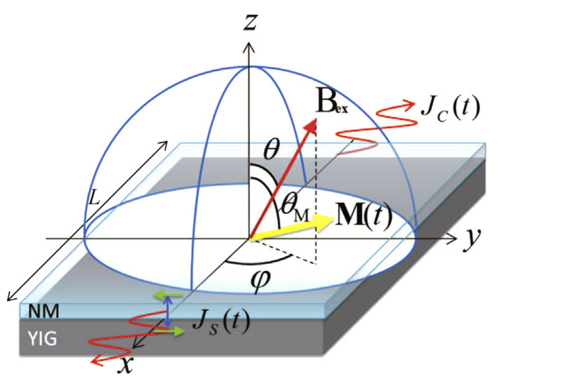

Fig. 1. Schematic of the device to observe the SMR rectified voltage in which an external magnetic field $\mathbf{B}_{\rm ex}$ is applied to the direction characterized by a polar angle θ and a azimuth φ while $\theta_{\rm M}$ shows the magnetization angles. The YIG(d_F nm)|N(d_N nm) bilayer film is patterned into a strip with a length L.

which the magnetization dynamics is excited by microwaves in coplanar wave guides or cavities. The ST-FMR magnetization is excited by spin Hall spin currents generated by an ac electric current bias (although Oersted magnetic fields may not be disregarded). An external magnetic field $\mathbf{B}_{\rm ex}$ is described by a polar angle θ and azimuth φ in the x–y plane. The magnetization dynamics can be expressed by the Landau–Lifshitz–Gilbert (LLG) equation with interface torques [5],

$$\partial_t \hat{\mathbf{M}} = -\gamma \hat{\mathbf{M}} \times \left(\mathbf{B}_{\rm eff} + \mathbf{b}_{\rm Oe}(t)\right) + \alpha \hat{\mathbf{M}} \times \partial_t \hat{\mathbf{M}} + \boldsymbol{\tau}_{ST}(t), \tag{1}$$

where $\mathbf{B}_{\rm eff} = \mathbf{B}_{\rm ex} + \mathbf{B}_{\rm dm} + \mathbf{B}_{\rm sm}(t)$ consists of the external magnetic field, the static demagnetizing field, and the dynamic demagnetization field, respectively. The Oersted field from the microwave current $\mathbf{b}_{\rm Oe}(t) = \mathbf{b}_{\rm Oe} e^{i(\omega_a t + \delta)}$ with frequency $\omega_a = 2\pi f_a$ and magnitude is determined by Ampère's Law (in the limit of an extended film) $b_{\rm Oe} = \mu_0 J_c^0 d_N/2$, where $J_c{}^0$ is an applied charge current density and δ the phase shift between Oersted field and current that is governed by the details of the sample design and therefore treated as an adjustable parameter [20]. The current-induced effective field generates the torque

$$\boldsymbol{\tau}_{ST}(t) = \gamma \left(b_{ST}^r \hat{\mathbf{M}} \times \hat{\mathbf{M}} \times \hat{\mathbf{s}} + b_{ST}^i \hat{\mathbf{M}} \times \hat{\mathbf{s}} \right) e^{i\omega_a t}, \tag{2a}$$

$$b_{ST}^{r(i)} = \frac{\hbar}{2|e|\mu_0 M_s d_F} \, \mathrm{Re}\left(\mathrm{Im}\right) \left[\eta \right] \theta_{\rm SH} J_c^0, \tag{2b}$$

where M_s and d_F are the saturation magnetization and thickness of the FI film, $\theta_{\rm SH}$ and $\hat{\mathbf{s}}$ the spin Hall angle and the direction (a unit vector) of the injected spin moment, and η the complex spin diffusion efficiency $\eta = g_S \tanh[d_N/(2\lambda)]/\left(1 + g_S \coth(d_N/\lambda)\right)$ with

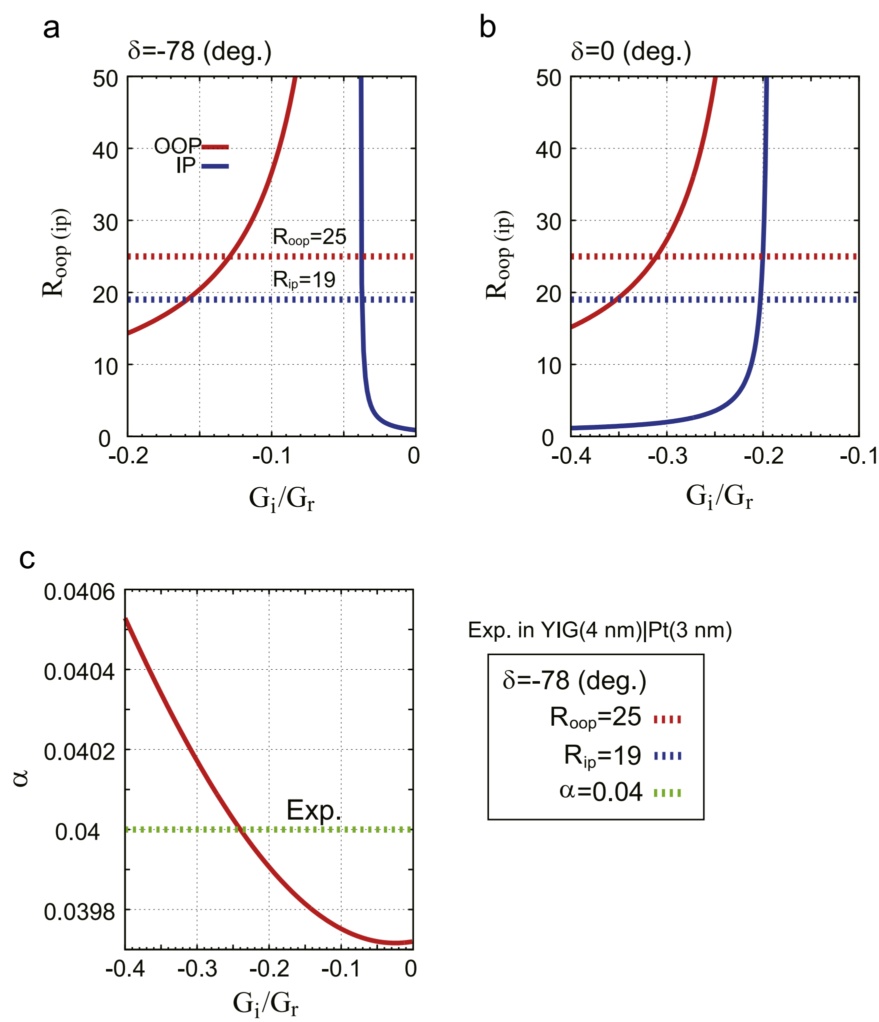

Fig. 2. (a)(b) The ratios of symmetric and antisymmetric contributions to the dc voltage for out-of-plane and in-plane magnetizations as a function of the G_i for (a) $\delta = -78°$ and (b) $\delta = 0°$. (c) The magnetization damping parameter α as a function of G_i. Dashed horizontal lines represent the experimental values for YIG(4 nm)|Pt(3 nm) [10]. $G_r = 4.0 \times 10^{14}\ \Omega^{-1}\,\mathrm{m}^{-2}$, $M_s = 128$ kA/m, $\gamma_0 = 1.76 \times 10^{11}\ \mathrm{T}^{-1}\,\mathrm{s}^{-1}$, $\alpha_0 = 8.58 \times 10^{-5}$ [21], $\theta_{\rm SH} = 0.11$, $\lambda = 1.5$ nm, and $\rho = 48.1\ \mu\Omega$ cm at $f_a = 7$ GHz are used for plotting.